PROCEEDINGS OF SCIENCE

Sub-barrier fusion of Si+Si systems : does the deformation of ^{28}Si play a role?

G. Colucci*, **G. Montagnoli, M. Faggian, A. Goasduff, M. Mazzocco, F. Scarlassara, C. Stefanini, E. Strano, M. Urbani**
Dipartimento di Fisica e Astronomia, Universitá di Padova, and INFN, I-35131 Padova, Italy.
E-mail: giulia.colucci@studenti.unipd.it

A. M. Stefanini, L. Corradi, E. Fioretto, F. Galtarossa†, G. L. Zhang
INFN, Laboratori Nazionali di Legnaro, I-35020 Legnaro, Italy.

D. Bourgin, S. Courtin, F. Haas
IPHC, CNRS-IN2P3, Université de Strasbourg, F-67037 Strasbourg Cedex 2, France.

P. Colovic, S. Szilner
Ruđer Bošković Institute, HR-10002 Zagreb, Croatia.

This contribution reports on the results of measurements of near- and sub-barrier fusion cross sections in the system ^{30}Si+^{30}Si performed at the Laboratori Nazionali di Legnaro of INFN.
The ^{30}Si beam of the XTU Tandem accelerator in the energy range of 47 - 90 MeV, was delivered on a metallic ^{30}Si target (50 μg/cm^2) enriched to 99.64 % in mass 30. A beam electrostatic deflector was used for the detection of evaporation residues.
The excitation function obtained for ^{30}Si+^{30}Si has been compared with the previous data on ^{28}Si+^{28}Si and Coupled Channels (CC) calculations using the M3Y+repulsion potential, taking into account the low lying 2^+ and 3^- excitations. Reproducing the low-energy ^{28}Si+^{28}Si excitation function was only possible by using a weak imaginary potential, probably simulating the oblate deformation of this nucleus. On the contrary, the data on ^{30}Si+^{30}Si are nicely reproduced by the CC calculations without any imaginary potential (^{30}Si has a spherical shape).
The astrophysical S-factor does not show a maximum, so that there is no evidence for hindrance in the measured energy range. The logarithmic derivative of the two excitation functions highlights the difference between the two systems. Even above the barrier the two systems behave differently. This is best seen by comparing the two barrier distributions where the high energy peak observed for ^{28}Si+^{28}Si is not found for ^{30}Si+^{30}Si. This is presumably due to the stronger couplings present in ^{28}Si and further theoretical analyses are in progress.

The 26th International Nuclear Physics Conference
11-16 September, 2016
Adelaide, Australia

*Speaker.
†Also Dipartimento di Fisica e Scienze della Terra, Univ. di Ferrara, Ferrara, Italy.

PoS(INPC2016)220

1. Introduction

Several experiments have shown that nuclear structure is very important in heavy ion fusion dynamics near the barrier. In order to clearly indicate this sensitivity, a valuable and often employed tool is the comparison of fusion data for neighboring isotopes.

Well-known results were obtained by comparing the fusion data for different nickel [1, 2] and calcium [3] isotopes, where the influence of transfer channels in fusion reactions was shown, or in the fusion of ^{16}O with different samarium isotopes [4, 5], where the change of the structure from spherical vibrational to strongly deformed nuclei was clearly observed.

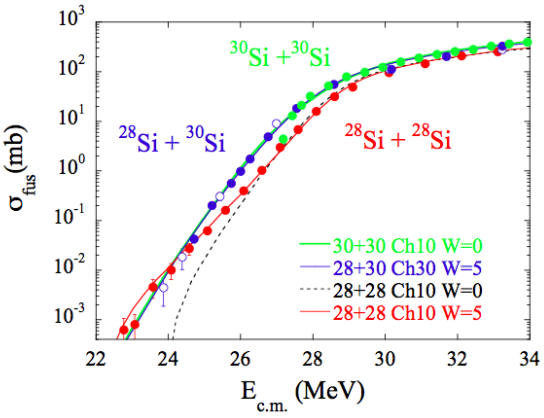

Figure 1: Measured fusion excitation functions of ^{28}Si+^{28}Si, ^{28}Si+^{30}Si [6] and previous data for ^{30}Si+^{30}Si [7]. The lines are the results of CC calculations (see text).

A comparative study of Si+Si systems [6] has revealed the influence of transfer on the fusion of the asymmetric case ^{28}Si+^{30}Si, well explained by including one- and successive two-neutron transfer channels in the coupling scheme, and highlighted a different behaviour of the two symmetric systems ^{28}Si+^{28}Si and ^{30}Si+^{30}Si (see Fig. 1) .

These systems are very interesting because of the different shape of the silicon isotopes: indeed ^{30}Si is nearly spherical, whereas ^{28}Si is strongly deformed with an oblate shape. The excitation function of ^{28}Si+^{28}Si has an unusual behavior, because the cross sections are hindered just below the barrier, but this effect disappears at lower energies. It was further surprising that the low-energy data were well reproduced only by artificially applying a weak, short-ranged imaginary potential, probably simulating the effect of the oblate deformation. This feature has to be further investigated and the present study of ^{30}Si+^{30}Si has been very significant in this respect.

No positive Q-value transfer channels are available in ^{30}Si+^{30}Si. This allows us to consider only couplings to vibrational states, neglecting the rotational ones which instead are present in the deformed nucleus ^{28}Si. This difference has an impact, as we shall see, on the energy dependence of fusion cross sections at sub-barrier energies for the two symmetric systems.

In view of all this, it is very tempting to compare the two reactions. Unfortunately the lack of experimental fusion data below 4 mb for ^{30}Si+^{30}Si prevented to perform a meaningful comparison and also to obtain information on the presence of hindrance phenomenon. A fusion experiment was then performed at the Laboratori Nazionali di Legnaro (LNL) of INFN with the purpose to extend the data on ^{30}Si+^{30}Si.

Here we present the results of this experiment on ^{30}Si+^{30}Si from well below to well above the Coulomb barrier and we compare the results with the previous data on ^{28}Si+^{28}Si.

2. Experimental set-up

Fusion cross sections can be determined by direct detection of the evaporation residues (ER). The ER, which are forward peaked, must be physically separated from the direct beam and the intense flux of elastically scattered beam particles. In order to achieve this separation at 0° and at small angles, an electrostatic field perpendicular to the direction of the particles is applied between the target and the detection system. Such an electrostatic beam deflector has been used in several sub- and near-barrier experiments at LNL and it was employed also in the study of ^{30}Si+ ^{30}Si fusion reaction.

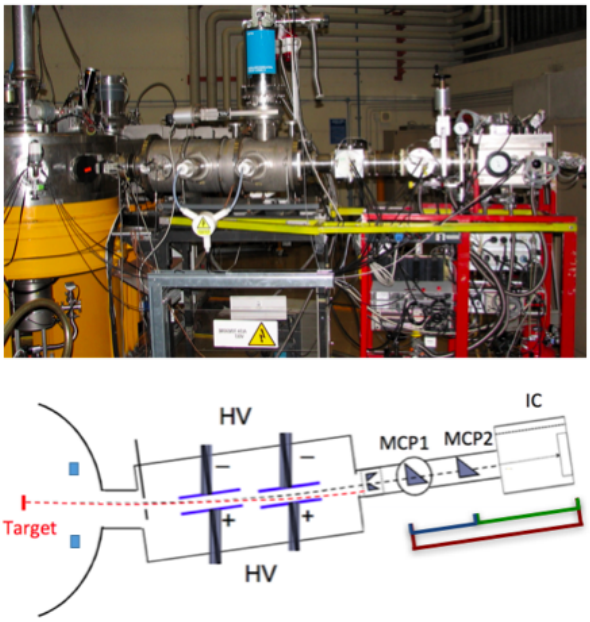

Figure 2: The experimental set-up (up) and its schematic design (down). The reaction chamber, the electrostatic deflector and the telescope E-TOF-ΔE are drawn from the left.

This set-up is shown in Fig. 2 and allows fast and reliable measurements of relative and absolute cross sections. The electrostatic deflector assures the separation of ER from the transmitted beam, while a subsequent E-TOF-ΔE telescope allows their identification. This telescope is made up of two micro-channel plates (MCP) detectors, a transverse field ionization chamber and a silicon detector placed in the same gas (CH_4) volume of the chamber. The ionization chamber provides a loss of energy signal ΔE, while the two MCPs yield the time of flights together with the silicon detector. In this configuration the silicon detector measures the residual energy of the ER and provides both the trigger for data acquisition and the start signal for the time of flight.

In Fig. 3 typical graphs reporting the time of flight (TOF) as a function of the residual energy E are shown. A good separation of ER events from the residual beam is achieved at energies both above and below the Coulomb barrier. Analogous two-dimensional spectra reporting the time of flight as a function of the loss of energy (ΔE) and the ΔE vs. residual energy were used in the data analysis. The sliding seal reaction chamber allows to measure angular distributions. In the reaction chamber four silicon detectors are placed symmetrically around the beam direction at the same scattering angle θ_{lab} = 16°. They are used to monitor the beam and normalize to the Mott scattering cross section. During the experiment three angular distributions were measured at the energies of 58, 72 and 80 MeV in the range from -6° to +9°. The total fusion cross sections were derived by integrating those distributions, and by simple interpolations or extrapolations for all other energies where ER measurements were taken only at 2° (or 3° for low energies).

The XTU Tandem accelerator in LNL provided ^{30}Si beams in the energy range of 47-90 MeV, with intensities of 15-30 pnA. The target consisted of 50 μg/cm^2 ^{30}Si evaporated on 30 μg/cm^2 carbon

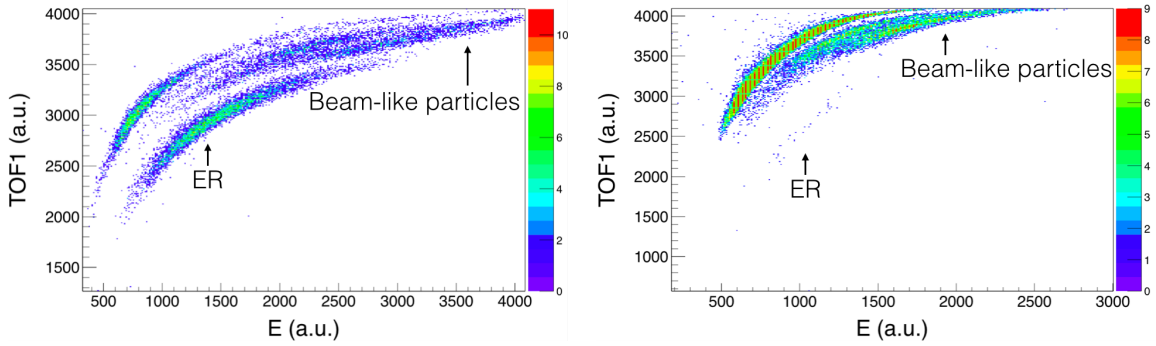

Figure 3: The graphs report the time of flight TOF1 (ordinate) as a function of the residual energy E (abscissa). The spectra were obtained above the Coulomb barrier (80 MeV, σ_{fus}=527 mb, left panel) and at a sub-barrier energy of 50 MeV (σ_{fus}=115 μb, right panel).

backings facing the beam. The isotopic enrichment of ^{30}Si was 99.64 %, where the small amounts of ^{29}Si and ^{28}Si did not affect the fusion cross section because of their higher Coulomb barriers with respect to ^{30}Si. The carbon backing and the silicon target introduced an average beam energy loss of around 750-850 keV, which was taken into account in the analysis.
The measured energy range allowed to extend the excitation function down to 4 μb, as shown Fig. 4 (left panel). The reported errors are statistical uncertainties, which reach a minimum value of 1-2 % at the higher energies and increase to 10-20 % at energies below the barrier. The systematic errors on the absolute cross section are of $\pm$ 7-8 %, due to the geometrical solid angle uncertainties, angular distribution integrations and mainly to the deflector transmission ($\sim$4 %).
The fusion cross sections of the two symmetric sistems are reported in Fig. 4 (right panel). The two excitation functions behave differently at low energies with a flatter slope for ^{28}Si+^{28}Si. A coupled channels analysis is necessary to understand the origin of this difference.

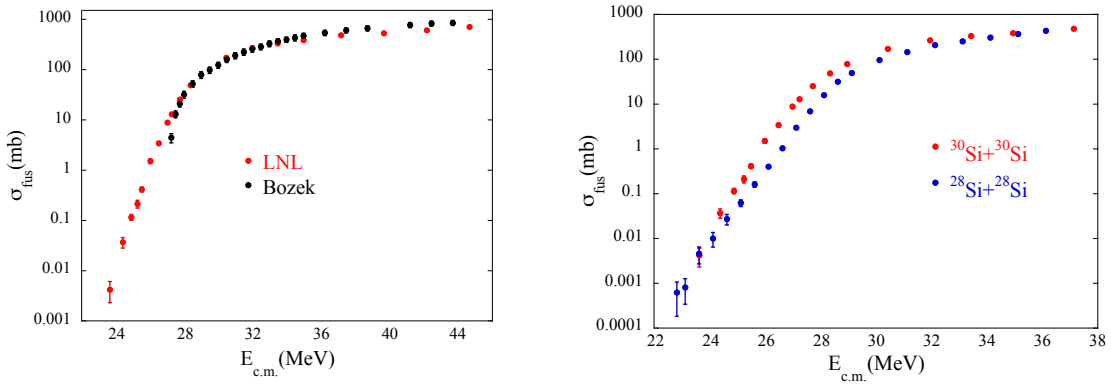

Figure 4: Fusion excitation function of ^{30}Si+^{30}Si compared to previous experimental data [7] (left panel) and to ^{28}Si+^{28}Si system (right panel).

3. Coupled Channel calculation

A preliminary coupled-channels (CC) analysis of the sub-barrier excitation function was per-

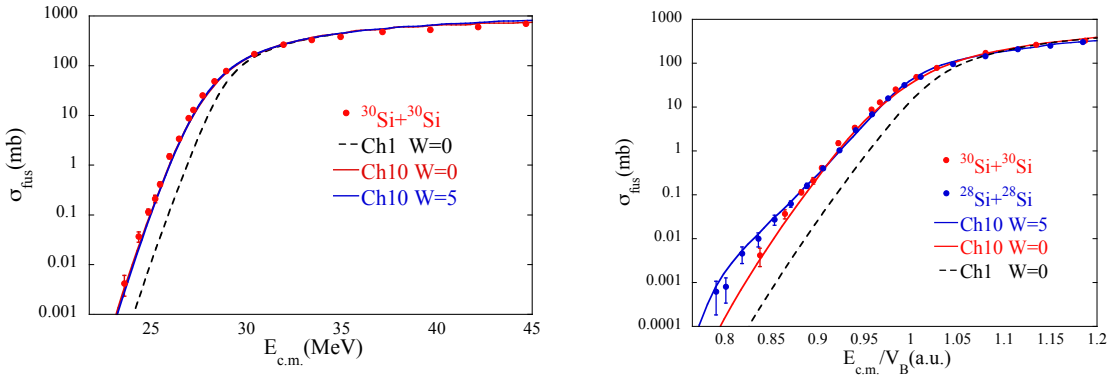

Figure 5: Fusion cross sections for ^{30}Si+^{30}Si compared to the no-coupling Ch1 calculation and to coupled-channels calculations at ten channels that are based on the predicted M3Y+rep potential with (Ch10 w5) and without (Ch10 w0) the addition of an imaginary potential (left panel). In the right panel the comparison with ^{28}Si+^{28}Si is reported including the coupled channel calculation adopted for this system, which employs a M3Y+rep potential with an imaginary part.

formed, using the M3Y+repulsion potential [8].

The CC calculations made use of the so-called isocentrifugal approximation, which simplifies the calculations by reducing the number of channels. The density of the ^{30}Si nucleus that determines the potential was adjusted to optimize the fit to the fusion data.

The complete CC calculation includes all one- and two-phonon excitations as well as mutual excitations of the low-lying 2^+ and 3^- states in both projectile and target, reaching a total of 15 channels. In order to simplify the calculations, the mutual excitation of the 2^+ and 3^- states in the same nucleus were ignored and so also the excitations of states above 10 MeV. These corrections allowed to neglegt the two-phonon and mutual excitations of the 3^- states and reduced the number of channels to 10 (refereed to as Ch10).

The ^{30}Si nucleus is nearly spherical, indeed the measured quadrupole moment of the 2^+ state is Q_2 = -0.05(6) barn, which is consistent with zero. This feature makes the calculation Ch10 more robust than in the other case because the location of minimum of channels potential is essentially the same in all channels, as it will be explained later. The adopted coupling strengths are shown in Table I of [6].

As shown in the previous section, the comparison of the excitation functions of ^{28}Si+^{28}Si and ^{30}Si+^{30}Si indicates a different behavior at energies below the Coulomb barrier. The reason for this was found [6] in the CC analysis for the two systems and originates in the shape of the two silicon isotopes. Indeed, the deformation makes the channel potentials for the excited states of the two nuclei very different. In the case of ^{28}Si the minimum of the potential for the 2^+ state is shifted to a smaller separation distance than the one observed in the entrance potential. In the case of ^{30}Si the minimum of all channel potentials are located essentially at the same separation distance. Since the incoming-wave boundary condition (IWBC) is imposed at the minimum of the entrance channel potential, this implies that for the system ^{28}Si+^{28}Si the fusion in the 2^+ channel is cut off at an energy that is higher than the minimum of the 2^+ channel potential, causing a suppression of the

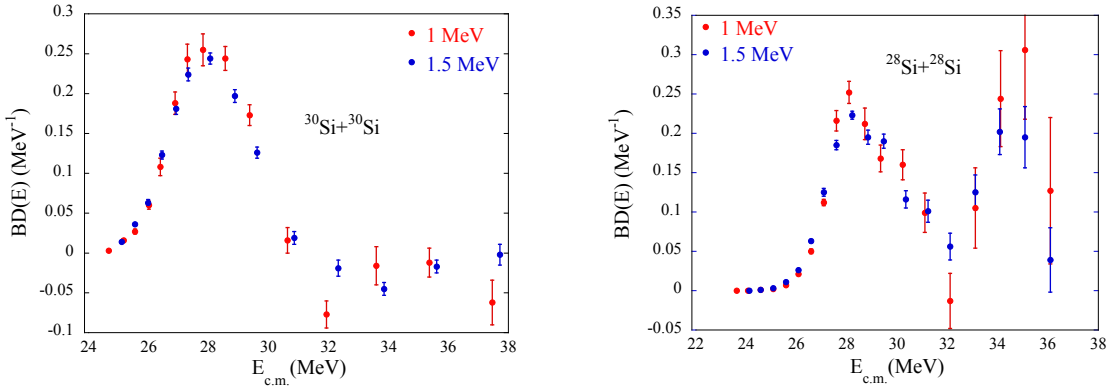

Figure 6: Barrier distribution extracted for ^{30}Si+^{30}Si (left panel) and ^{28}Si+^{28}Si (right panel) system, with energy steps of 1.0 MeV (red points) and 1.5 MeV (blue points).

calculated cross sections at low energies. By applying a weak imaginary potential it was possible to reproduce the low-energy data. On the contrary, beacuse of the spherical shape of ^{30}Si, the IWBC is imposed at the minimum of each channel potential, providing a more consistent treatment of the fusion in the different reaction channels. As a consequence, there is no need for an imaginary potential at low energy. This is shown in Fig. 5 where the results of CC calculation without and with the imaginary potential are reported. One sees that there is essentially no difference between the two calculations.

4. Barrier distribution

The evaluation of the barrier distribution [9] for the ^{30}Si+^{30}Si system and its comparison with the one of ^{28}Si+^{28}Si is very useful in order to obtain more information on the role of the deformation of ^{28}Si. The barrier distributions were obtained using the three-point difference formula [10], with two energy steps of 1.0 MeV and 1.5 MeV, and a meaningful difference between the two cases has been observed. The ^{30}Si+^{30}Si system shows a single well-defined peak at low energies (Fig. 6, left panel), while a double-peak structure appears for ^{28}Si+^{28}Si with a clearly defined peak at higher energies (Fig. 6, right panel). These dissimilar behaviours arise from the different structures of the two nuclei and from the stronger couplings present in ^{28}Si+^{28}Si due to the oblate shape of ^{28}Si.

5. Hindrance

The hindrance phenomenon is a suppressions of fusion cross sections with respect to standard CC calculations, occurring far below the Coulomb barrier [11, 12]. The investigation of this effect usually makes use of two representations of the excitation functions, i.e. the astrophysical S-factor [13] and the logarithmic derivative L(E), which allow to reveal the presence of hindrance without using model calculations. Indeed, the S factor shows a maximum vs. energy in the presence of hindrance at the energy where the logarithmic slope L(E) reaches the value L_{CS} expected for a constant astrophysical S factor.

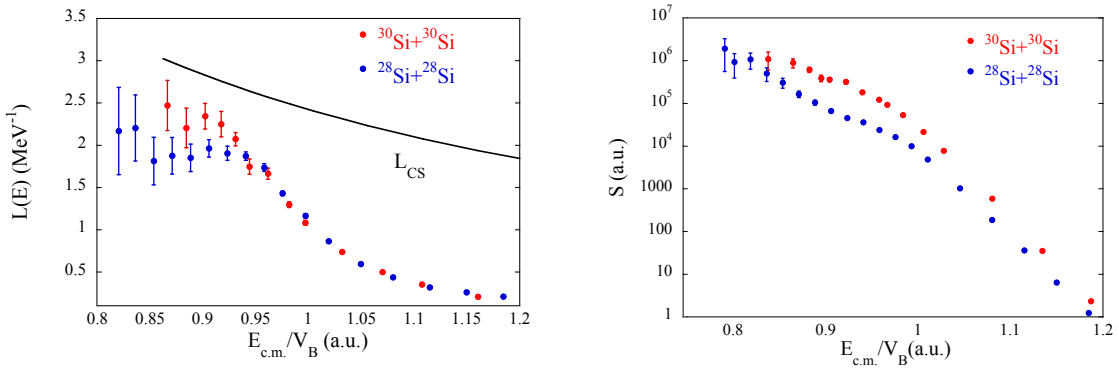

Figure 7: In the left panel the logarithmic derivative of the excitation function of the two symmetric systems is reported, where L_{CS} (black line) is the slope expected for a constant astrophysical S-factor. The S-factor extracted from experimental data for both cases is reported in the right panel.

The investigation of hindrance in the ^{30}Si+^{30}Si fusion reaction is interesting also because the Q-value for the fusion of this system is positive. It has been pointed out that in such cases the S factor does not necessarily develop a maximum [12]. In the case of ^{30}Si+^{30}Si the S factor does not show any maximum vs. energy (see Fig. 7, right panel), even if it appears to saturate at the lowest measured energies. The logarithmic derivative does not cross the L_{CS} curve (left panel). This allows us to conclude that there is no evidence of hindrance down to around 4 μb.
The ^{28}Si+^{28}Si system shows a different behavior of the S factor and the slope. Indeed, there is evidence of hindrance at energies slightly below the Coulomb barrier [6] but the effect disappears at lower energies. On the other hand, the logarithmic derivative saturates far below the barrier.

6. Summary

The fusion excitation function of ^{30}Si+^{30}Si has been measured in a wide energy range down to 4 μb. In this range there is no evidence for hindrance, when observing the logarithmic slope and S-factor. The comparison with ^{28}Si+^{28}Si shows that the two systems behave differently both near the barrier (the high energy peak observed in the barrier distribution of ^{28}Si+^{28}Si is not found for ^{30}Si+^{30}Si) and farther below, where the regular trend of the heavier system can contrasted with the unusual one of ^{28}Si+^{28}Si. The weaker couplings in ^{30}Si+^{30}Si and its spherical shape make the difference. This is confirmed by coupled-channels calculations using the M3Y potential that are in good agreement with experimental data. At variance with the case of ^{28}Si+^{28}Si, the addition of a weak short-ranged imaginary potential is not necessary to reproduce the sub-barrier energy fusion cross sections.

7. Acknowledgments

We are very grateful to the XTU Tandem staff and to M.Loriggiola for preparing targets of excellent quality. This work has been supported in the part by the Croatian Science Foundation under the project 7194.

References

[1] M. Beckerman, M. Salomaa, A. Sperduto, J. D. Molitoris, and A. Di Rienzo, *Sub-barrier fusion of ^{58,64}Ni with ^{64}Ni and ^{74}Ge*, Phys. Rev. C **25** (1982) 837.

[2] M. Beckerman et al., *Dynamic Influence of Valence Neutrons upon the Complete Fusion of Massive Nuclei*, Phys. Rev. Lett. **45** (1980) 1472.

[3] G. Montagnoli et al., *Fusion of ^{40}Ca+^{40}Ca and other Ca+Ca systems near and below the barrier*, Phys. Rev. C **85** (2012) 024607.

[4] R. Stokstad et al., *The sub-barrier fusion of ^{40}Ar with ^{144,148,154}Sm*, Z. Phys. A **295** (1980) 269.

[5] H. Esbensen, *Fusion and zero-point motion*, Nucl. Phys. A **352** (1982) 147.

[6] G. Montagnoli et al., *Fusion of ^{28}Si+^{28,30}Si: Different trends at sub-barrier energies*, Phys. Rev. C **90** (2014) 044608.

[7] E. Bozek et al., *De-excitation of ^{58,60,62}Ni compound nuclei formed via symmetric and asymmetric entrance channels*, Nucl. Phys. A **451** (1986) 171.

[8] Ş. Mişicu and H. Esbensen, *Signature of shallow potentials in deep sub-barrier fusion reactions*, Phys. Rev. C **75** (2007) 034606.

[9] N. Rowley, G. R. Satchler, and P. H. Stelson, *On the "distribution of barrier" interpretation of heavy-ion fusion*, Phys. Lett. B **254** (1991) 25.

[10] H. Timmers et al., *A case study of collectivity, transfer and fusion enhancement*, Nucl. Phys. A **633**, (1998) 421.

[11] C. L. Jiang, et al., *Unexpected Behavior of Heavy-Ion Fusion Cross Sections at Extreme Sub-Barrier Energies*, Phys. Rev. Lett. **89** (2002) 052701.

[12] C. L. Jiang, H. Esbensen, B. B. Back, R. V. F. Janssens, and K. E.Rehm, *Analysis of heavy-ion fusion reactions at extreme sub-barrier energies*, Phys. Rev. C **69** (2004) 014604.

[13] E.Margaret Burbidge, G.R. Burbidge, William A. Fowler and F. Hoyle, *Synthesis of the Elements in Stars*, Rev. Mod. Phys. **29** (1957) 547.